ADVANCED MATERIALS

[23] Z. Y. Jiang, Z. X. Xie, S. Y. Xie, X. H. Zhang, R. B. Huang, L. S. Zheng, *Chem. Phys. Lett.* **2003**, *368*, 425.
[24] H. Y. Zhang, Z. Q. Hu, K. Lu, *Nanostruct. Mater.* **1995**, *5*, 41.
[25] Y. Suzuki, A. Okamoto, M. Yoshitake, S. Ogawa, *Nucl. Instrum. Methods Phys. Res. Sect. B* **1997**, *121*, 107.
[26] Z. Hao, Y. Wu, Y. Enomoto, K. Tanabe, N. Koshizuka, *J. Cryst. Growth* **2002**, *235*, 253.
[27] V. K. Tikhomirov, P. Hertogen, G. J. Adriaenssens, C. Glorieux, R. Ottenburgs, *J. Non-Cryst. Solids* **1998**, *227*, 732.
[28] Z. Y. Tang, N. A. Kotov, M. Giersig, *Science* **2002**, *297*, 237.
[29] H. Dai, E. W. Wong, Y. Z. Lu, S. Fan, C. M. Lieber, *Nature* **1995**, *375*, 769.
[30] C. R. Martin, *Science* **1994**, *266*, 1961.

Polymer-Mediated Alignment of Carbon Nanotubes under High Magnetic Fields**

By *Hamid Garmestani*,* *Marwan S. Al-Haik*, *Klaus Dahmen*, *Rina Tannenbaum*, *Dongsheng Li*, *Simon S. Sablin*, and *M. Yousuff Hussaini*

Carbon nanotubes possess exceptional mechanical properties and superior thermal and electric properties.[1–4] Hence, nanotubes can be ideal reinforcement fibers for structural composites. For example, a cast composite film consisting of polystyrene and carbon nanotubes (5 % volume fraction) has increased the modulus by 100 % and the strength of the polystyrene by 25 %.[5] Moreover, the carbon nanotubes reinforcement increased the toughness of the composite by absorbing energy because of their high elastic behavior during loading.[5] Utilizing the unique properties of carbon nanotubes depends on the spatial control and dispersion of individual nanotubes in a matrix, such as polymers, and on the ability to transfer load from the matrix to the nanotubes.

The fabrication of high-performance nanotube-based composites is driven by the ability to create anisotropy at the molecular level in order to obtain optimal mechanical properties. Oriented single-walled carbon nanotubes (SWCNTs) offer many advantages compared to the random tangles of bundled tubes.[6] Recently, multi-walled carbon nanotubes were dispersed in a polystyrene matrix followed by extrusion and pressing the composite film to produce oriented nanocomposites,[7] in which the elastic modulus was considerably greater than the improvement for the randomly oriented composite.

Carbon nanotubes have been aligned through different techniques such as hot filament chemical vapor deposition,[8] melt processing,[9] mechanical stretching,[10] and electrophoresis.[11] However, when introduced into a polymeric matrix, carbon nanotubes disperse randomly, losing their orientations. Hence, the reorientation process should take into consideration the rearrangement of the polymeric matrix. Bulk orientation for polymers was shown to occur via extensional shear obtained by melt spinning,[12] extrusion,[13] or injection molding.[14–16] Magnetic field-induced alignment of polymeric materials has been the focus of several research efforts.[17–22] Polymers can interact with a magnetic field through the diamagnetic anisotropy of its constituent repeating units. The energy that the repeating unit gains through the interaction with an external magnetic field is dependent on the orientation of the unit relative to the magnetic field, and hence, the unit tends to align in a certain direction that optimized the energy reduction.[21] If the energy reduction is insufficient compared to its thermal energy, the tendency of a unit to align is suppressed by molecular vibrations. Magnetic reorientation of various polymers has been measured by X-ray diffraction,[16,17,21,23] magnetic birefringence,[20] nuclear magnetic resonance (NMR),[24] and by studying the evolution of microstructures.[17,22,25,26] The application of a magnetic field during polymer processing may achieve enhanced mechanical and physical properties compared to mechanical stretching.[16,17,25,26] For example, a magnetic field was applied during the cure reaction of a liquid crystalline epoxy,[16,17] resulting in alignment of the molecules along the direction of the applied field. Measurements of the orientation parameter of the fully cured material by wide-angle X-ray scattering (WAXS) showed that orientation improved with an increase in field strength. The orientation parameters attained a maximum level at field strength of approximately 12 T. The elastic tensile modulus increased with the square of the orientation parameter, attaining a maximum value of 8.1 GPa, compared to 3.1 GPa for the unoriented material. The authors have reported the improvement in mechanical properties (Young's Modulus, Universal Hardness) and physical properties (thermal conductivity, electrical conductivity, susceptibility) elsewhere.[27,28]

Although there are many investigations of polymer orientation under a magnetic field, there are only few studies reporting the alignment of a second phase inside the polymer, such as fibers,[23] nanoparticles,[29,30] and nanotubes.[6,30] In the polymer–nanotube system, the alignment is based on the different magnetic properties of the two materials. The reorientation of carbon nanotubes in a polymeric medium occurs due to the cooperative effect of the magnetic torque exerted by the magnetic field directly on the nanotubes and by the hydrodynamic torque and viscous shear (i.e., drag forces) exerted on the nanotubes by the polymer chains.

[*] Prof. H. Garmestani, Dr. M. S. Al-Haik, Dr. D.-S. Li
Department of Mechanical Engineering
FAMU-FSU College of Engineering
Tallahassee, FL 32310 (USA)
E-mail: hamid.garmestani@mse.gatech.edu
Prof. H. Garmestani, Prof. R. Tannenbaum
School of Materials Science and Engineering
Georgia Institute of Technology
Atlanta, GA 30332 (USA)
Dr. K. Dahmen
Suntrans Inc.
Tallahassee, FL 32306 (USA)
Dr. S. S. Sablin, Prof. M. Y. Hussaini
School of Computational Science and Information Technology
Florida State University
Tallahassee, FL 32306 (USA)

[**] The major funding for this research was provided as part of a grant from the Army Office of research DAAD19-01-1-0742. This work was performed at the NHMFL, Tallahassee Florida. The authors gratefully acknowledge the experimental assistance of the pulsed magnet group and Robert Guddard from the material characterization group. Additional funding (for R. T.) was also provided by the AFOSR-MURI program on Structural Energetic Materials.

  DOI: 10.1002/adma.200304932 *Adv. Mater.* **2003**, *15*, No. 22, November 17

The microstructures of magnetically untreated and magnetically processed samples have been examined using environmental scanning electron microscopy (ESEM). Fracture surfaces were prepared by fracturing across the alignment direction on planes parallel to the magnetic field orientation. The micrographs of the fracture surface of the epoxy samples are presented in Figure 1. The fracture surface of the sample processed outside the magnetic field shows no preferred orientation (Fig. 1a). The application of a 15 T magnetic field led to the development of domains, within which the chains of the epoxy polymer are oriented in the direction of the field. The magnetically developed morphology of the epoxy takes fibril shape (Fig. 1b). The optical orientation of the domains appears to be relatively uniform, with the exception of slight changes at the boundary wall. However, for the sample processed under 25 T magnetic field (Fig. 1c), the fibrils are more uniform along the direction of the magnetic field, and all domains, including the boundary, show a common orientation aligning efficiently with the field. It is clear that the preferred orientation induced by the 15 and 25 T fields is very apparent in the fracture surface morphology of the samples, which is facile on planes parallel to the magnetic field direction. Where fracture is induced across the magnetic field axis, the crack path frequently jumps planes, giving a wedge appearance to the fracture surface as seen in Figure 1b,c.

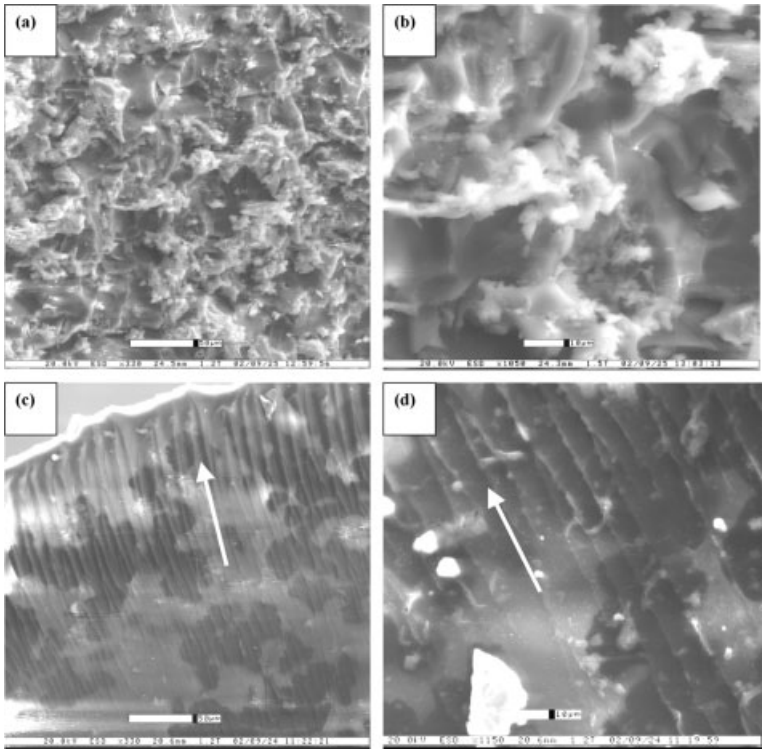

Fig. 2. ESEM images for the morphology of the fracture surface of SWCNT–epoxy composite. The fracture surface processed at 0 T magnetic field was captured at two magnifications: scale bar representing a) 50 μm and b) 10 μm. The fracture surface processed at 25 T magnetic field was also captured at two magnifications: scale bar representing c) 50 μm and d) 10 μm. The arrow is the direction of the magnetic field. The darkest spots are clusters of the carbon nanotubes intercalated along the polymer fibrils.

In the carbon nanotube composite samples, the corresponding fracture surfaces were similarly produced and imaged using ESEM. The fracture surface for the composite sample processed outside the field is shown in Figure 2a,b. The addition of 3 wt.-% SWCNTs to the epoxy produced a fracture surface that is very rough compared to that of the epoxy alone, but both samples do not exhibit any preferred orientation. The processing of the epoxy composite under a 25 T magnetic field produced a uniform fracture surface, where the epoxy fibrils are aligned along the direction of the field, and the SWCNTs are the dark spots in the dispersed phase along these fibrils, as shown in Figure 2c,d. The use of a 25 T magnet easily generated fibril formation in the epoxy, but did not guarantee the alignment of the SWCNTs along the magnetic field orientation, especially considering the smaller scale of the nanotubes compared to the polymer fibrils. The magnetically processed nanocomposite sample was sliced into thin films (10 μm thick) and was investigated using the atomic force microscope (AFM). At a relatively low magnification, the ropes of nanotubes look relatively dispersed (Fig. 3, left), but at a higher magnification (Fig. 3, right), bundles of SWCNTs are locally aligned in the direction parallel to the

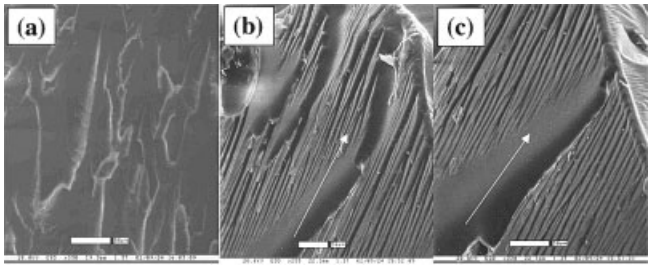

Fig. 1. ESEM images for the morphology of the fracture surfaces for the magnetically processed epoxy samples at a) 0 T, b) 15 T, and c) 25 T. All the samples where processed using the same curing schedule: 2 h at 25 °C then 4 h at 60 °C. The arrows represent the direction of the corresponding applied magnetic field. The scale bars represent 50 μm.

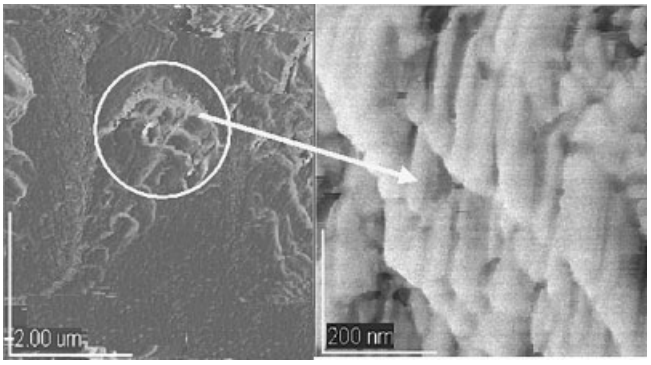

Fig. 3. AFM microscopy for the SWCNT–epoxy composite cured inside a 25 T magnetic field. The curing time temperature cycle was 2 h at 25 °C, followed by 2 h at 60 °C. The image on the right represents the enhanced detail of the encircled area in the image on the left.

ADVANCED MATERIALS

25 T magnetic field. The degree of alignment achieved in the magnetically oriented sample is encouraging. Beside the magnetic anisotropy of the carbon nanotubes, the highly aligned epoxy will facilitate the alignment of carbon nanotubes along the direction of the magnetic field.

It is commonly understood that the amorphous chains segments can have some local order. Wide-angle X-ray diffraction (WAXD) is used for confirmation of the amorphous chain segments short to medium range ordering. In the current investigation, WAXD was used to measure the orientation distribution of the polymer chain axes rather than measuring the distance between these chains. The 2θ scans for three different epoxy samples at $\phi = 0°$, are shown in Figure 4a. From the figure it is clear that there are no significant peaks that could be attributed to crystalline lamellae, but only a weak diffuse halo that can be attributed to the amorphous regions of the epoxy resin. The analysis of this halo can provide information concerning the structure of the amorphous regions. The position of the halo is at $2\theta = 19°$, corresponding to a period distance of 4.7 Å, which is related to the average interchain distance in the amorphous component. The decrease in the intensity of the peak as the magnetic field strength increases, indicates that

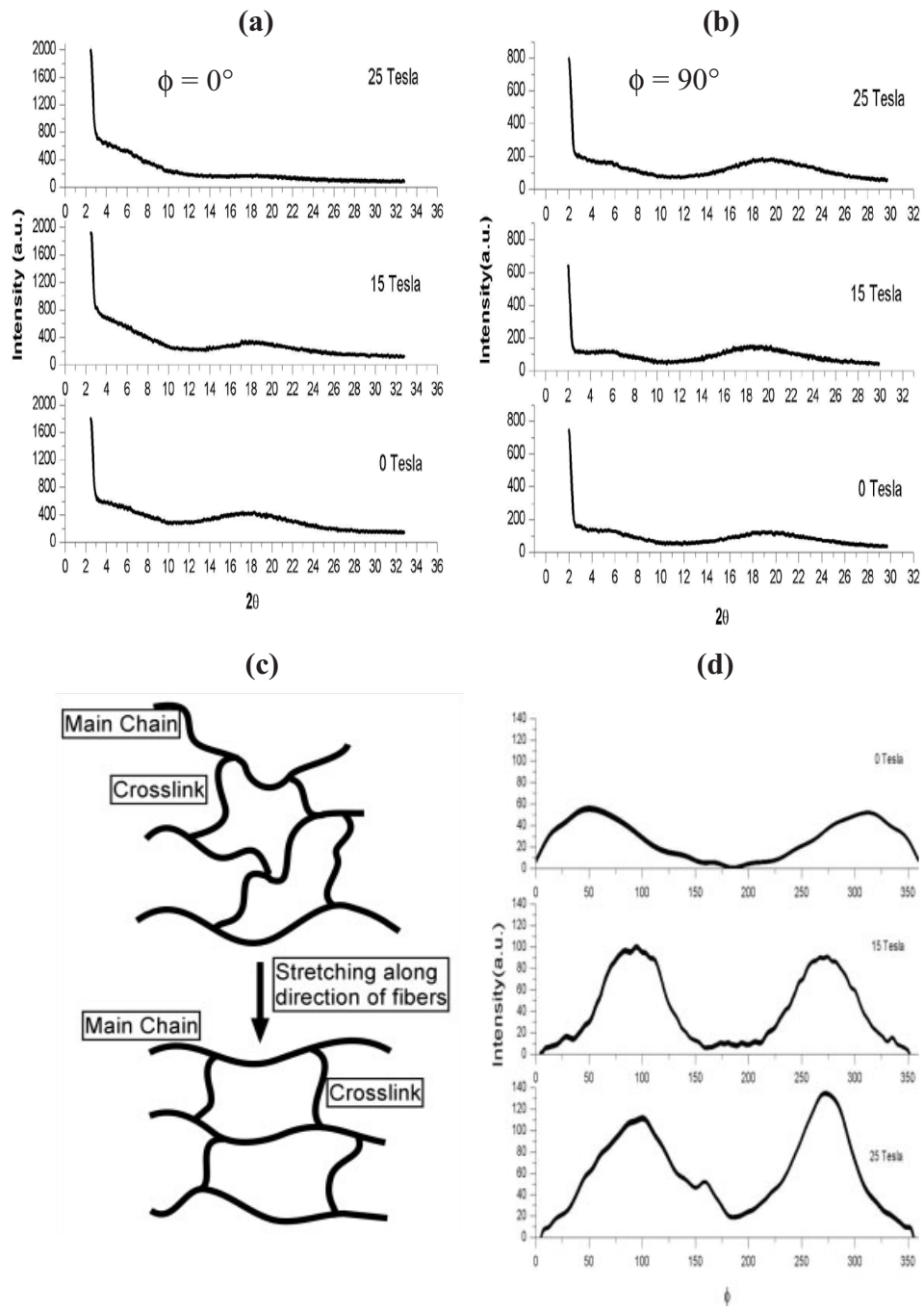

Fig. 4. a) 2θ diffraction along the azimuthal direction ($\phi = 0°$, normal to the magnetic field direction) for the 0 T, 15 T, and 25 T cured epoxy samples. b) 2θ diffraction along the azimuthal direction ($\phi = 90°$, parallel to the magnetic field direction) for the 0 T, 15 T, and 25 T cured epoxy samples. Note that these samples do not contain SWCNTs. c) The two-dimensional stretching effect that the magnetic field exerts on the crosslinked epoxy. d) Azimuthal (ϕ) scans of diffraction intensity for different magnetically processed epoxy samples. All scans carried out for fixed $2\theta = 19°$.

the magnetic field minimized the orientation density along the transverse direction of the samples, at $\phi = 0°$. For $\phi = 90°$ the diffraction scans give information about the orientation of the amorphous chains along the axis of the sample that was parallel to the applied magnetic field, as shown in Figure 4b. The results of the scan along the sample axis suggest that the increase in the magnetic field strength forced the amorphous phase to reorient along the magnetic field direction, and hence this reorientation is more pronounced at $2\theta = 19°$. This is most likely due to the two-dimensional stretching effect that the magnetic field exerts on the crosslinked epoxy network, as shown schematically in Figure 4c.

The change in the intensity of the amorphous peak signifies that the amorphous chain segments, locally reoriented parallel to the sample axis, are more densely packed than those that are either randomly oriented or oriented perpendicular to the sample axis. The peak of the amorphous halo increases proportional to the increment in the magnetic field strength. To study the alignment of the amorphous phase, comprehensive azimuthal scans were measured by fixing 2θ value at 19° and varying θ in the range $0° \leq \phi < 360°$ for each magnetically processed sample as shown in Figure 4d. It can be seen that all three ϕ scans contain a set of two peaks, and that the peaks in all scans are located at the same angle at around $\phi = 90°$ and 270° with a separation of 180°. The obvious feature in the azimuthal intensity scans of the amorphous diffraction is the increase of the halo intensity with the increase of the magnetic field strength, and the narrowing of the peak's width, measured as full width at half maximum (FWHM). This confirms the reorientation of the amorphous chains along the axial direction of the sample that was parallel to the applied magnetic field.[31]

The above-mentioned in-plane orientation relationships are in good agreement with previous studies of epoxy resin systems cured under magnetic fields,[18,21] in which it was found that the presence of the magnetic field during the cure reaction aligned the molecules along the applied field. In these studies, orientation parameters obtained from WAXS patterns show that orientation reached maximum level at field strength of approximately 12 T. Even though the epoxy resin used in our system is different, the alignment behavior of the molecules under that magnetic field is very similar. Our ϕ scans show that the molecules oriented along the magnetic direction, and that the degree of orientation generated in the system is at its highest at a field strength of 25 T.

Experimental

Thixotropic epoxy was used as the matrix (PTM&W industries, Inc., brand name PR2032), and together with a PH3660 hardener, the system cures at room temperature for 24 h. SWCNTs were provided by Carbon Nanotechnologies, Inc. The SWCNTs were dispersed ultrasonically in the thixotropic/PR2032 epoxy resin before curing. The components were mixed using a high intensity ultrasonic processor to promote the distribution of carbon nanotubes over the surface of the resin and prevent particle clustering. The hardener was added with stirring to the resin and the resin–carbon nanotube mixture. The mix ratio for each sample was 4:1 by weight. The epoxy–nanotube system had 3 wt.-% carbon nanotubes. The liquid systems were degassed moderately until no gas bubbles could be seen, then injected separately, using 10 mm syringes, into quartz tubes ($D_{in} = 8$ mm and $L = 50$ mm), which were sealed and wrapped around a sample holder using non-magnetic tape.

Magnetic processing of the samples was carried out at the National High Magnetic Field Laboratory (NHMFL). The magnetic fields used were generated by a 25 T direct current (DC) resistive solenoid. The sample holder was placed in a furnace, which was pushed into the large magnet bore, such that the samples were in the center of the magnetic field. Once the magnetic field was generated, the sample was left to cure at room temperature inside the field for 2 h with no applied heat, to keep the viscosity as low as possible. Then the furnace was heated up to 60 °C, and the sample was left to cure under the magnetic field for another 2 h. Subsequently, the magnetic field was reduced to 0 T and the samples were placed in another furnace at 60 °C for another 2 h to fully cure. The experiment was repeated at 15 T field with the same magnetic processing and curing cycles.

The fracture surfaces were examined by an Electroscan Model E-3 ESEM environmental scanning electron microscope. Morphology of the epoxy–carbon nanotubes specimen surface was observed using a tapping mode AFM on a JSPM 4210 instrument, equipped with an Olympus silicon tip (type AC160TS-C2) oscillating slightly below its resonance frequency (~300 kHz). WAXD measurements were obtained on a Philips X'Pert PW 3040 MRD X-ray diffractometer equipped with a pole figure goniometer employing Ni filtered Cu Kα radiation. The accelerating voltage was 50 kV and the tube current was 40 mA. The 2θ scan data were collected from $2\theta = 1°$ to 30° in 0.01° steps for a period of 1 s per step. A series of radial scans were obtained at various azimuthal angles (ϕ) by rotating the sample on its own plane between $\phi = 0°$ and $\phi = 360°$. ϕ scans were performed in 0.1° steps for a period of 0.5 s per step.

Received: January 29, 2003
Final version: July 11, 2003

[1] S. Iijima, *Nature* **1991**, *354*, 56.
[2] D. Qian, E. C. Dickey, *J. Microsc.* **2001**, *204*, 39.
[3] J. Bernholc, M. B. Nardelli, V. Meunier, C. Roland, *Annu. Rev. Mater. Res.* **2002**, *32*, 347.
[4] E. T. Thostensona, Z. Renb, T. W. Choua, *Comp. Sci. Technol.* **2001**, *61*, 1899.
[5] B. Safadi, R. Andrews, E. A. Grulke, *J. Appl. Polym. Sci.* **2002**, *84*, 2660.
[6] B. W. Smith, Z. Benes, D. E. Luzzi, J. E. Fischer, D. A. Walters, M. J. Casavant, J. Schmidt, R. E. Smalley, *Appl. Phys. Lett.* **2000**, *77*, 663.
[7] E. T. Thostenson, W. Chou, *J. Phys. D* **2002**, *35*, 77.
[8] Y. Chen, L. Guo, S. Patel, D. T. Shaw, *J. Mater. Sci.* **2000**, *35*, 5517.
[9] R. Haggenmueller, H. H. Gommans, A. G. Rinzler, J. E. Fischer, K. I. Winey, *Chem. Phys. Lett.* **2000**, *330*, 219.
[10] L. Jin, C. Bower, O. Zhoua, *Appl. Phys. Lett.* **1998**, *73*, 1197.
[11] K. Yamamoto, S. Akita, Y. Nakayama, *Jpn. J. Appl. Phys.* **1996**, *35*, 917.
[12] X. Yuan, A. F. Mak, K. W. Kwok, B. Yung, K. Yao, *J. Appl. Polym. Sci.* **2001**, *81*, 251.
[13] J. H. Greenblatt, D. Fensom, *J. Ind. Eng. Chem.* **1911**, *39*, 1037.
[14] G. Kalay, M. J. Bevi, *J. Poly. Sci., Part B: Polym. Phys.* **1997**, *35*, 265.
[15] I. Heynderickx, F. Paridaans, *Polymer* **1993**, *34*, 4068.
[16] D. M. Lincoln, E. P. Douglas, *Polym. Eng. Sci.* **1999**, *39*, 1903.
[17] B. C. Benicewicz, M. E. Smith, J. D. Earls, R. D. Priester, Jr., S. M. Setz, R. S. Duran, E. P. Douglas, *Macromolecules* **1998**, *31*, 4730.
[18] T. Kimura, T. Kawi, Y. Sakamoto, *Polymer*, **2000**, *41*, 809.
[19] T. Kawai, Y. Sakamoto, T. Kimura, *Mater. Trans. JIM* **2000**, *41*, 955.
[20] H. Ezure, T. Kimura, S. Ogawa, E. Ito, *Macromolecules* **1997**, *30*, 3600.
[21] S. A. Kossikhina, T. Kimura, E. Ito, M. Kawahara, *Polym. Eng. Sci.* **1997**, *37*, 396.
[22] A. Anwer, A. H. Windle, *Polymer* **1993**, *34*, 3347.
[23] H. E. Assender, A. H. Windle, *Polymer* **1997**, *38*, 677.
[24] T. Kimura, M. Yamato, W. Koshimizu, M. Koike, T. Kawai, *Langmuir* **2000**, *16*, 858.
[25] F. Volino, A. Martins, R. J. Blumstein, *Phys. Lett.* 1**981**, *42*, 305.
[26] S. A. Kossikhina, T. Kimura, E. Ito, M. Kawahara, *Polym. Eng. Sci.* **1998**, *38*, 914.
[27] E. S. Choi, J. S. Brooks, D. L. Eaton, M. S. Al-Haik, H. Garmestani, K. Dahmen, *Appl. Phys.*, in press.
[28] M. S. Al-Haik, H. Garmestani, R. Tannenbaum, K. Dahmen, *J. Polym. Sci., Part B: Polym. Phys.*, in press.
[29] T. A. Man'ko, E. A. Dzhur, F. P. Sanin, M. Ermoleav, *Mech. Compos. Mater.* **2001**, *37*, 171.
[30] S. Sun, S. Anders, H. F. Hamann, J. U. Thiele, J. E. E. Baglin, T. Thomson, E. E. Fullerton, C. B. Murray, B. D. Terris, *J. Am. Chem. Soc.* **2002**, *124*, 2884.
[31] The field-assisted reorientation of the epoxy samples induced the alignment of the carbon nanotubes at the nanoscale level, while the carbon nanotubes ropes did not align globally due to their length.

